TITLE

Diffusion-Weighted Magnetic Resonance Imaging in Peritoneal Carcinomatosis from Ovarian Cancer: Diagnostic performance in correlation with surgical findings.

AUTHORS:

1. **Javier Garcia Prado, MD [a, d] CORRESPONDING AUTHOR**

   Email: fjgarcia@mdanderson.es

   Telephone number: +34 678 456 411 Fax number: +34 91 768 06 81

2. **Concepción González Hernando, MD, PhD [b, c]**

   Email: cghernando@salud.madrid.org

3. **David Varillas Delgado, PhD, BQ [d]**

   Email: david.varillas@ufv.es

4. **Raquel Saiz Martínez, MD [a]**

   Email: rsaizmtnez@hotmail.com

5. **Priya Bhosale, MD [e]**

   Email: Priya.Bhosale@mdanderson.org

6. **Javier Blazquez Sanchez, MD [a]**

   Email: jblazquez@mdanderson.es

7. **Luis Chiva, MD, PhD [f, g]**

   Email: lchiva@unav.es

[a] Department of Radiology. MD Anderson Cancer Center. C/ Arturo Soria 270, 28033-Madrid, Spain.

[b] Department of Radiology. Hospital Universitario Puerta de Hierro – Majadahonda. C/ Manuel de Falla 1 28222 – Majadahonda – Madrid, Spain.

[c] Universidad Autónoma de Madrid (UAM) Medicine School
C/ Arzobispo Morcillo 4, 28029 Madrid, Spain.

[d] Francisco de Vitoria University (UFV), Faculty of Health Sciences, Research Unit, Carretera Pozuelo-Majadahonda km 1.800 28223 Pozuelo de Alarcón (Madrid), Spain.

[e] Department of Radiology. MD Anderson Cancer Center. 1400 Pressler Street, FCT 15.6038 Houston, TX 77030, United States of America.

[f] Department of Gynecology. Clínica Universitaria de Navarra. C/ Marquesado de Sta. Marta, 1, 28027 - Madrid, Spain.

[g] University of Navarre, Medicine School, Department of Gynecology -Director, C/ Irunlarrea 1. 31008 Pamplona. Navarra, Spain.

ABSTRACT

INTRODUCTION:

Ovarian Cancer (OC) is the first death cause by gynaecological cancer in developed countries and the third cause of gynaecological cancer in the world.

Detecting irresectable disease is crucial to select surgical candidates and Peritoneal Carcinomatosis (PC) depiction helps to get a complete debulking without residual disease >1cm, the best prognostic predictor in advanced OC.

CT is the elective technique for abdominal imaging, although its accuracy for PC in OC and cytoreduction success prediction ability is limited. PET/CT is considered for systemic evaluation in OC however, it is not a reference standard for PC.

PC presents as high signal foci in DWI, with higher contrast than conventional MRI. Whole Body DWI with Background Suppression MRI (WB-DWIBS/MRI) combines conventional anatomic with Diffusion Weighted Imaging (DWI).

This study aims to assess the diagnostic performance and tumour burden correlation of WB-DWIBS/MRI in ovarian PC using PCI, referred to cytoreduction surgery as standard reference.

MATERIAL AND METHODS:

Our local ethical board approved this prospective study and all participants signed written informed consent. 50 out of 217 consecutive patients with disseminated primary or recurrent OC were eligible for cytoreduction and WB-DWIBS/MRI.

Peritoneal Cancer Index (PCI) scores (0-3) tumour burden in 13 anatomical regions, hence global ranging 0-39. Two radiologists (R1 and R2) preoperatively assessed PCI and the gynaecologic-oncologist team after.

Diagnostic performance was calculated for each of the PCI regions and globally. We evaluated interobserver agreement using Cohen´s Kappa, statistic differences with the

McNemar test (significativity $p<0.05$) and tumour burden with Pearson correlation test for R1 and R2.

RESULTS:

Histology was epithelial OC in 72% (36/50) and complete cytoreduction was achieved in 39/50 patients. Correlation test was 0.762 ($p<0.001$) for R1 and R2 0.642 ($p<0.001$). Global diagnostic performance was Sensitivity 0.84; Specificity 0.89; positive predictive value 0.72; negative predictive value 0.92; Accuracy 0.89; Kappa 0.41.

DISCUSION:

Global tumour burden was low (average PCI 7). Pelvis and right hypochondrium showed the highest positive rate and diagnostic performance. The intestinal regions presented the lowest positive rate.

Although only a few used PCI, previous studies reported similar results than ours with higher Sensitivity when compared to CT and PET/CT.

CONCLUSION:

WB-DWIBS/MRI is a reliable imaging technique to preoperatively quantify and depict PC of ovarian origin in order to get a complete cytoreductive surgery.

KEYWORDS:

Peritoneal carcinomatosis

MR imaging

Ovarian cancer

Whole-body magnetic resonance imaging (WB-MRI)

Diffusion weighted imaging (DWI)

Diffusion-weighted whole-body imaging with background body signal suppression (DWIBS)

ABBREVIATIONS

OC Ovarian Cancer

PC Peritoneal Carcinomatosis

PCI Peritoneal Cancer Index

CT Computed Tomography

PET/CT Positron Emission Tomography CT with 18-fluorodeoxyglucose

HIPEC Hyperthermic Intraperitoneal Chemoperfusion

DWI Diffusion Weighted Imaging

WB-DWIBS/MRI Whole Body DWI with Background Suppression MRI

INTRODUCTION

Ovarian Cancer (OC) is the first death cause by gynaecological cancer in developed countries and it is globally the third cause of gynaecological cancer, with an incidence of 3412 and a 5-year prevalence for general population 7939 for 2017 in Spain, similar to other industrialized countries [1, 2]. The most common OC histology is epithelial, and up to 65% are diagnosed at stages III and IV with Peritoneal Carcinomatosis (PC) and nodal dissemination, with high mortality associated [2, 3].

Treatment of choice in epithelial OC is primary surgical cytoreduction followed by platinum-based adjuvant chemotherapy [4]. Achieving a complete surgical debulking, without residual disease >1cm (R0), is the best prognostic predictor in advanced OC [5]. Occasionally, if primary surgery cannot be initially performed [5], an interval surgery after 3 cycles of neoadjuvant chemotherapy might be considered. Secondary cytoreduction is the surgery after recurrence, if there is an option for R0 debulking.

Preoperative detection of irresectable disease is crucial to select surgical candidates, the detection and location of peritoneal seeding in OC is useful for planning an accurate surgery.

Laparoscopy has been proposed as a preoperative evaluation using the Fagotti score [6]. This system assesses 8 peritoneal structures and assigns a score 0-2. If global scoring is ≥8, then the predictive positive value (PPV) of a suboptimal surgical result is 100%. However, laparoscopy is an invasive technique, and it cannot evaluate the retroperitoneum nor the tumour posterior to the gastrosplenic ligament and in the lesser sac [7].

Peritoneal Cancer Index (PCI) [8] was described for PC quantification in surgical cytoreduction and Hyperthermic Intraperitoneal Chemoperfusion (HIPEC).

PCI is a region-wise scoring system that assesses 13 anatomic regions with a range 0-3 each, attending the largest lesion in each region (No tumour LS0; up to 0.5 cm LS 1; up to 5 cm LS 2 and more than5 cm or confluent LS 3) (Fig.2) thereby was calculated as the addition of all regional scoring in each patient, with a total burden range from 0 to 39.

PCI is used in digestive carcinomatosis candidates for cytoreduction and HIPEC, and not so often in ovarian carcinomatosis given that the only accepted prognostic factor is a complete debulking without residual disease >1cm, whereas HIPEC is still under discussion in advanced OC [9].

Currently, no imaging tool is capable of predicting the success of a complete resection.

Different imaging techniques are used in preoperative PC assessment describing several dissemination patterns [10, 11].

Due to its availability and reproducibility, Computed Tomography (CT) is the central imaging technique for abdominal imaging and when using a dedicated protocol, CT correlates well with surgical PCI [12].

CT is recommended for staging and restaging for gynaecologic malignancies by American College of Radiology (ACR) and National Comprehensive Cancer Network (NCCN) guidelines. CT accuracy for PC in OC and capability for predicting success of cytoreductive surgery is limited, although when evaluated with CA-125 it may predict prognosis [13, 14].

Positron Emission Tomography CT with 18-fluorodeoxyglucose (PET/CT) can be considered for systemic evaluation in gynaecologic malignancies, especially in OC although it is not yet stablished as a reference standard when compared to CT for PC depiction [15].

Conventional MRI is useful in peritoneal carcinomatosis [16], however it is inferior to PET/CT [17, 18] and similar to CT [19].

Diffusion Weighted Imaging (DWI) is obtained by using high-energy short-time MR radiofrequency pulses, *b* value expresses the strength of potentiation in diffusion. Using high *b* values (*b* max.≥ 1000) DWI provide very high signal intensity of structures with water movement restriction that can be pathologic (tumour, blood and others) or not (lymph nodes, nervous structures…) and almost no signal of the rest of the anatomy.

Dynamic contrast-enhanced imaging and DWI improve the capability of tumour pelvic recurrence characterization [20] and adding high *b* DWI to routine MRI, raises the diagnostic performance for peritoneal metastases [21-24].

When DWI is combined with conventional imaging of the entire body for anatomic reference and characterization of findings, we obtain Whole Body DWI with Background Suppression MRI (WB-DWIBS/MRI) images [25].

This study aims to assess the diagnostic performance and tumour burden correlation of WB-DWIBS/MRI in ovarian PC using PCI, referred to cytoreduction surgery as standard reference.

MATERIAL AND METHODS

Study design

This is an observational prospective single-institutional non-comparative diagnostic performance study of WBMRI/DWIBS versus pathologic proven surgical standard of reference. Institutional review board approval was obtained, and all patients signed written informed consent.

Study population

Inclusion criteria were: Suspected diagnosis of primary or recurrent ovarian carcinoma by CA-125 raise and imaging findings. Exclusion criteria were: Claustrophobia, known renal impairment (Creatinine > 1.5 mg/dl or glomerular filtration rate <60 ml/min/1.73m^2), contraindications to hyoscine butyl-bromide (allergies, glaucoma, history of bowel obstruction or urinary retention), non-operable patients and non-resectable disease [7]. Patients considered for interval debulking surgery were not considered for the study.

From June 2014 to January 2017, 217 consecutive patients presented in our institution and were evaluated in interdisciplinary meeting, 108 were considered for initial chemotherapy and 109 were candidates for cytoreduction and they were offered to undergo a WBMRI/DWIBS exam. 61 patients met all the inclusion criteria (Fig. 1), 11 were not evaluated by both radiologists, therefore 50 were finally considered for the

study. Any positive finding on WBMRI/DWIBS which would preclude surgery was biopsied.

Imaging protocol

Patients drank 1 litre of pure pineapple juice 2 hr before as a negative oral contrast agent. We injected 20 mg diluted in 100 cc saline solution hyoscine butyl-bromide, 50 cc at the beginning of the examination and the other 50 cc before the DWIBS sequence. Intravenous contrast gadobutrol 1 mmol/ml (0, 2 ml/kg weight) was given at an injection rate 2ml/s (MEDRAD® Spectris Solaris EP Injection System).

Imaging was performed on a 1.5 T system (Ingenia, Philips Healthcare, Best, The Netherlands) (Table 1) with head/neck and two body phased-array coils for anatomic covering from head to mid thighs [26] [25].

Coronal and axial single-shot T2 –weighted turbo spin echo (T2TSE) and volumetric 3DT1-weighted fat sat gradient-echo (3DT1GE) for anatomic evaluation and DWIBS imaging (*b*-values: 0 and 1000 s/mm^2) were obtained in the coronal plane.

In a dedicated MR workstation (IntelliSpace Portal. Version 606.20039, Philips Medical Systems Nederland B.V.), we obtained reformatted Maximum Intensity Projection (MIP) images in the axial and sagittal planes and colour derived maps using T2TSE and 3DT1GE as a reference layer and DWIBS MIP-DWIBS as a colour functional overlay (alpha blending 50%).

Imaging analysis

Two radiologists (R1 and R2 with 10 and 5 years in abdominal imaging respectively) read the same 50 examinations, both blinded to medical history and the other radiologist findings.

Tumour detection was assessed with DWIBS and the findings were correlated with T2TSE and 3DT1GE sequences for anatomic location.

Any size nodular, plaque or linear intrabdominal high signal foci on DW were considered positive and documented for every region (13) in each patient, based on PCI. If a nodule was detected in conventional images but showed no signal in DWI, it was considered positive. Peritoneal surface contrast enhancement, ascites or adhesions were not considered as peritoneal tumour. We did not evaluate Apparent Diffusion Coefficient (ADC) given the small size of some implants.

Both radiologists used the PCI (Fig. 2) [8] for assessing regional diagnostic performance in 50 cases.

Standard of reference

OC treatment naïve patients with indication for surgical resection were considered to undergo primary cytoreduction, and those who had prior surgery were considered to undergo non-primary cytoreduction.

All the patients were operated by the same gynaecologic surgeon and general surgeon. The same two pathologists evaluated all samples. All the pathologists and surgeons had more than 15 years each in gynaecologic oncology.

Regions were assessed during surgery according to the PCI system and specimens were labelled for subsequent pathological confirmation.

Statistical analysis:

SPSS v21.0 software (IBM) was used with *p*-values <0.05 indicating statistical significance. WBMRI/DWIBS findings were compared with surgery obtaining sensitivity, specificity, positive predictive value (PPV), negative predictive value and

accuracy. Statistic differences between both techniques were calculate with the two-tailed McNemar test and in order to avoid biases Bonferroni correction was used.

Cohen Kappa statistic was used to evaluate interobserver agreement (κ <0.2, Slight; <0.4, Fair; <0.6, Moderate; <0.8, Substantial; >0.8 Perfect). Surgical and preoperative global PCI was assessed with correlation Pearson test.

RESULTS

A total of 50 patients were selected for the study and peritoneal seeding was pathologically confirmed after surgery in 13 PCI regions (Fig 2)

Table 2 shows the clinical outcome. Surgery was delayed in some patients due to acute comorbidities (acute infections, renal impairment and others).

Almost all the patients (94%, 47/50) presented primary gynaecologic disease, 88% (44/50) were primary gynaecologic malignancies and 76% (38/50) were of ovarian origin and histology was epithelial in 72% (36/50).

Figure 3 presents the frequency of disease detected in each region and Table 3 diagnostic performance of WBMRI/DWIBS for R1 and R2.

The global average surgical PCI was 7.42 ± 5.675, 7.08 ± 5.865 for R1 and for R2, 7.06 ± 5.245. Pearson correlation test was 0.762 ($p<0.001$) for R1 and R2 0.642 ($p<0.001$) (Figure 4).

Overall positive scoring (Score values 1-3) for surgical findings, R1, and R2 were 28.46%, 30.77 and 24.15% respectively (Fig. 5)

Global diagnostic performance was calculated as the average of regional performances presented statistical significance ($p<0.05$) for both observers when compared with surgery, except for specificity (Table 3).

Interobserver agreement is globally fair to moderate although it is moderate to substantial in 6 out of 13 regions evaluated.

Regional evaluation showed that pelvis presented the highest number of positives for both observers and surgery, with a high sensitivity although a moderate specificity. Central region is the second with highest rate of positives with a moderate sensitivity and high specificity for both observers.

Central region and bowel loops show a low detection rate, although they present a good diagnostic performance.

Accuracy is over 0.86 in all the regions for R1 and above 0.8 in 6/13 regions for R2 and global accuracy is 0.89 and 0.8 respectively.

DISCUSSION:

This prospective study evaluated the diagnostic performance and tumour burden quantification using WB-DWIBS/MRI in ovarian PC, using imaging PCI referred to surgical PCI in patients undergoing primary or secondary cytoreduction. Those patients receiving interval debulking surgery after 3 cycles of chemotherapy were excluded of the study, given that tumour necrosis and bleeding might be a false positive source [27]. Secondary cytoreduction is a different clinical situation, they are patients that recurred sometime after primary surgery therefore, it can be considered new disease.

We adopted PCI [8] as a reproducible mean for PC distribution and tumour burden quantification for different imaging techniques [12, 14, 16, 28-33] and surgical findings; others evaluated WB-MRI/DWIBS regional ovarian carcinomatosis [24, 26, 34-37] attending non-PCI anatomical compartments, so local assessment is difficult to compare given the variations in classifications, although global evaluation can be useful.

Global tumour burden was low (average PCI 7) and most of the regions showed no peritoneal implants because many of the patients with high tumour burden did not fulfil operability or resectability criteria, therefore they were not eligible for this study.

We found a significative correlation in peritoneal tumour burden of MRI compared with surgery, that is better than reported for PET/CT or CT [15].

Pelvis followed by right hypochondrium, showed the highest positive rate and diagnostic performance. The first because it is the site of the primary tumour and peritoneal implants deposit by gravity effect, and the second because of the high contrast of the tumour with the liver surface (Fig. 6), whose signal is almost null in DWIBS, compared to the lack of density differences in CT or PET/CT.

The intestinal regions presented the lowest positive rate because massive affection may preclude surgical resection if it obliges to multiple anastomosis. The central zone showed a variable positive rate, partly because mesentery root infiltration may also contraindicate surgery and because omental infiltration is difficult to assign in one of these compartments. Moreover, assignation of a lesion to one or another compartment was sometimes challenging.

WB-DWIBS/MRI global and regional accuracies are statistically significative, with good values although there are regional variations.

Our results are in line with previous studies. To the best of our knowledge, only one study evaluated ovarian carcinomatosis with WB-DWIBS/MRI using PCI [31] with higher Sensitivity when compared to CT and PET/CT, however in a fifteen-patient sample.

Other studies assessing gynaecological cancer with DWIBS provided similar results, with better diagnostic performance than CT, although with variable designs, sample sizes and different regional evaluation than PCI [26, 34-37].

Our diagnostic performance in region 5 overlaps with the recently described for splenic infiltration [38] both for CT and MRI. The findings can be partially explained by the physiologic high DWI signal of the spleen, that may difficult tumour detection. However, splenic infiltration does not preclude cytoreduction and miliary carcinomatosis and different key peritoneal regions must be evaluated.

When compared to PET/CT, WB-DWIBS/MRI shows better [26, 37] or at least similar [23, 31] diagnostic performance for PC. Some studies provided better results for PET/CT, though MR did not combine DWI sequences [17] neither they were considered in some initial meta-analysis [18]. However, more recent ones reported better performance than PET/CT when using WB-DWIBS/MRI [39].

Our regional sensitivites are very close to the reported [21, 30-31] when evaluating WB-DWIBS/MRI with PCI for local diagnostic performance, although with higher specificities in almost every region, probably because the use of higher b values (b1000), except pelvis that also showed better sensitivity.

One limitation is that this is a single institutional study. There can be an occult selection bias since the patients selected for the study were also candidates for cytoreduction, so that resectability itself and areas that may contraindicate resectability might be underevaluated.

Although patients undergoing interval-debulking surgery were excluded, more than half of the sample are postoperated patients, therefore diagnostic performance may have been affected. T2-Shine-through may be a source of false positive findings in DWIBS sequence, especially in dense fluids such as blood, mucin or coagulative necrosis that keep hyperintense signal in high *b* DWIBS imaging [27] but they can be confirmed with other sequences (T2 or T1*-contrast enhanced). Another major limitation is that we did not directly compare WB-DWIBS/MRI with other imaging techniques such as CT or

PET/CT, given that patients were referred by different institutions, with various initial modalities and wide variations in imaging protocols.

However, this is a prospective nature study of a moderately large very homogeneous sample where almost all patients were OC, and we present a quantitative approach of imaging findings related to surgery.

Even though it is out of the scope of this study, WB-DWIBS/MRI can evaluate nodal and supradiaphragmatic dissemination.

Given that ADC was not evaluated, further research may be needed to stablish a cutoff point for DW signal intensity similarly to standard uptake value (SUV) in PET/CT.

As a conclusion, WB-DWIBS/MRI is a reliable imaging technique helpful to preoperatively quantify and depict peritoneal carcinomatosis in ovarian cancer in order to get a complete cytoreductive surgery.

TABLES AND FIGURES:

Table 1: Sequence protocol of WB-DWIBS/MRI. DWIBS, Diffusion Weighted Imaging with Background Suppression; 3DT1GE, 3D volumetric Gradient Echo T1; THRIVE T1-weighted High Resolution Isotropic Volume Examination; SPAIR Spectrally Adiabatic Inversion Recovery; mDIXON multi-echo 2-point DIXON.

Table 2: Clinical characteristics and outcome in the patients included.

Table 3: Global and regional diagnostic performance of WB-DWIBS/MRI for both observers (R1 and R2) and surgery.

Figure 1: Flowchart showing the sample selection criteria for the study.

Figure 2: PCI diagram.

Figure 3: Percentage of positives detected in the different peritoneal regions using PCI system, with WB-DWIBS/MRI for observers R1 (a, d) and R2 (b, e) compared with surgery (c, f).

Figure 4: Correlation between surgical total PCI (vertical axis) and WB-DWIBS/MRI total PCI (horizontal axis) for R1 (a) and R2 (b).

Figure 5: Bar chart shows overall PCI score distribution considering 650 (13 × 50) observations.

Figure 6: Coronal native images weighted in T2TSE (a), 3DGET1 (b) and DWIBS (c) and red-scale DWIBS fused imaging with T2 (d) 3DGET1 (e) in the same planes as above and in para-aortic plane (f).

Asterisks show ascites in both flanks and pelvis. Peritoneal carcinomatosis (white arrowheads) is shown in flanks, greater omentum, subdiaphragmatic and perihepatic spaces, left hypochondrium and pelvis surrounding ascites. Para-aortic and pericaval lymph nodes (black arrows) and supraclavicular node (white arrow) are depicted.

REFERENCES

[1]https://seom.org/seomcms/images/stories/recursos/Las_Cifras_del_cancer_en_Espana2018.pdf

[2] L.A. Torre, B. Trabert, C.E. DeSantis, K.D. Miller, G. Samimi, C.D. Runowicz, M.M. Gaudet, A. Jemal, R.L. Siegel, Ovarian cancer statistics, 2018: Ovarian Cancer Statistics, 2018, CA: A Cancer Journal for Clinicians. 68 (2018) 284–296. doi:10.3322/caac.21456.

[3] WHO classification of tumours of female reproductive organs - NLM Catalog - NCBI, (n.d.). https://www.ncbi.nlm.nih.gov/nlmcatalog/101656343 (accessed December 5, 2018).

[4] T. Thigpen, The if and when of surgical debulking for ovarian carcinoma, N. Engl. J. Med. 351 (2004) 2544–2546. doi:10.1056/NEJMe048292.

[5] I. Vergote, C.G. Tropé, F. Amant, G.B. Kristensen, T. Ehlen, N. Johnson, R.H. Verheijen, M.E. van der Burg, A.J. Lacave, P.B. Panici, others, Neoadjuvant chemotherapy or primary surgery in stage IIIC or IV ovarian cancer, N. Engl. J. Med. 363 (2010) 943–953.

[6] A. Fagotti, G. Ferrandina, F. Fanfani, G. Garganese, G. Vizzielli, V. Carone, M.G. Salerno, G. Scambia, Prospective validation of a laparoscopic predictive model for optimal cytoreduction in advanced ovarian carcinoma, Am. J. Obstet. Gynecol. 199 (2008) 642.e1–6. doi:10.1016/j.ajog.2008.06.052.

[7] S. Nougaret, H.C. Addley, P.E. Colombo, S. Fujii, S.S. Al Sharif, S.H. Tirumani, K. Jardon, E. Sala, C. Reinhold, Ovarian Carcinomatosis: How the Radiologist Can Help Plan the Surgical Approach, Radiographics. 32 (2012) 1775–1800. doi:10.1148/rg.326125511.

[8] P.H. Sugarbaker, Review of a personal experience in the management of carcinomatosis and sarcomatosis, Jpn. J. Clin. Oncol. 31 (2001) 573–583.

[9] L.M. Chiva, A. Gonzalez-Martin, A critical appraisal of hyperthermic intraperitoneal chemotherapy (HIPEC) in the treatment of advanced and recurrent ovarian cancer, Gynecol. Oncol. 136 (2015) 130–135. doi:10.1016/j.ygyno.2014.11.072.

[10] S. González-Moreno, L. González-Bayón, G. Ortega-Pérez, C. González-Hernando, Imaging of peritoneal carcinomatosis, Cancer J. 15 (2009) 184–189. doi:10.1097/PPO.0b013e3181a58ec3.

[11] F. Iafrate, M. Ciolina, P. Sammartino, P. Baldassari, M. Rengo, P. Lucchesi, S. Sibio, F. Accarpio, A. Di Giorgio, A. Laghi, Peritoneal carcinomatosis: imaging with 64-MDCT and 3T MRI with diffusion-weighted imaging, Abdom Imaging. 37 (2012) 616–627. doi:10.1007/s00261-011-9804-z.

[12] M.A. Mazzei, L. Khader, A. Cirigliano, N. Cioffi Squitieri, S. Guerrini, B. Forzoni, D. Marrelli, F. Roviello, F.G. Mazzei, L. Volterrani, Accuracy of MDCT in the preoperative definition of Peritoneal Cancer Index (PCI) in patients with advanced ovarian cancer who underwent peritonectomy and hyperthermic intraperitoneal chemotherapy (HIPEC), Abdom Imaging. 38 (2013) 1422–1430. doi:10.1007/s00261-013-0013-9.

[13] R.S. Suidan, P.T. Ramirez, D.M. Sarasohn, J.B. Teitcher, S. Mironov, R.B. Iyer, Q. Zhou, A. Iasonos, H. Paul, M. Hosaka, C.A. Aghajanian, M.M. Leitao Jr., G.J. Gardner, N.R. Abu-Rustum, Y. Sonoda, D.A. Levine, H. Hricak, D.S. Chi, A multicenter prospective trial evaluating the ability of preoperative computed tomography scan and serum CA-125 to predict suboptimal cytoreduction at primary debulking surgery for advanced ovarian, fallopian tube, and peritoneal cancer, Gynecologic Oncology. 134 (n.d.) 455–461. doi:10.1016/j.ygyno.2014.07.002.

[14] D. Diaz-Gil, F.J. Fintelmann, S. Molaei, A. Elmi, S.S. Hedgire, M.G. Harisinghani, Prediction of 5-year survival in advanced-stage ovarian cancer patients based on computed tomography peritoneal carcinomatosis index, Abdom Radiol (NY). 41 (2016) 2196–2202. doi:10.1007/s00261-016-0817-5.

[15] V. Lopez-Lopez, P.A. Cascales-Campos, J. Gil, L. Frutos, R.J. Andrade, M. Fuster-Quiñonero, E. Feliciangeli, E. Gil, P. Parrilla, Use of (18)F-FDG PET/CT in the preoperative evaluation of patients diagnosed with peritoneal carcinomatosis of ovarian origin, candidates to cytoreduction and hipec. A pending issue, Eur J Radiol. 85 (2016) 1824–1828. doi:10.1016/j.ejrad.2016.08.006.

[16] B. Klumpp, P. Aschoff, N. Schwenzer, I. Koenigsrainer, S. Beckert, C.D. Claussen, S. Miller, A. Koenigsrainer, C. Pfannenberg, Correlation of preoperative magnetic resonance imaging of peritoneal carcinomatosis and clinical outcome after peritonectomy and HIPEC after 3 years of follow-up: preliminary results, Cancer Imaging. 13 (2013) 540–547. doi:10.1102/1470-7330.2013.0044.

[17] B.D. Klumpp, N. Schwenzer, P. Aschoff, S. Miller, U. Kramer, C.D. Claussen, B. Bruecher, A. Koenigsrainer, C. Pfannenberg, Preoperative assessment of peritoneal carcinomatosis: intraindividual comparison of 18F-FDG PET/CT and MRI, Abdom Imaging. 38 (2013) 64–71. doi:10.1007/s00261-012-9881-7.

[18] P. Gu, L.-L. Pan, S.-Q. Wu, L. Sun, G. Huang, CA-125, PET alone, PET-CT, CT and MRI in diagnosing recurrent ovarian carcinoma: a systematic review and meta-analysis, Eur J Radiol. 71 (2009) 164–174. doi:10.1016/j.ejrad.2008.02.019.

[19] C.M.C. Tempany, K.H. Zou, S.G. Silverman, D.L. Brown, A.B. Kurtz, B.J. McNeil, Staging of Advanced Ovarian Cancer: Comparison of Imaging Modalities—Report from the Radiological Diagnostic Oncology Group, Radiology. 215 (2000) 761–767. doi:10.1148/radiology.215.3.r00jn25761.

[20] E. Sala, A. Rockall, D. Rangarajan, R.A. Kubik-Huch, The role of dynamic contrast-enhanced and diffusion weighted magnetic resonance imaging in the female pelvis, Eur J Radiol. 76 (2010) 367–385. doi:10.1016/j.ejrad.2010.01.026.

[21] R.N. Low, C.P. Sebrechts, R.M. Barone, W. Muller, Diffusion-Weighted MRI of Peritoneal Tumours: Comparison With Conventional MRI and Surgical and Histopathologic Findings—A Feasibility Study, AJR. 193 (2009) 461–470. doi:10.2214/AJR.08.1753.

[22] M. Bozkurt, S. Doganay, M. Kantarci, A. Yalcin, S. Eren, S.S. Atamanalp, I. Yuce, M.I. Yildirgan, Comparison of peritoneal tumour imaging using conventional MR imaging and diffusion-weighted MR imaging with different b values, Eur J Radiol. 80 (2011) 224–228. doi:10.1016/j.ejrad.2010.06.004.

[23] G. Manenti, C. Cicciò, E. Squillaci, L. Strigari, F. Calabria, R. Danieli, O. Schillaci, G. Simonetti, Role of combined DWIBS/3D-CE-T1w whole-body MRI in tumour staging: Comparison with PET-CT, European Journal of Radiology. 81 (2012) 1917–1925. doi:10.1016/j.ejrad.2011.08.005.

[24] J.M. Winfield, N.M. deSouza, A.N. Priest, J.C. Wakefield, C. Hodgkin, S. Freeman, M.R. Orton, D.J. Collins, Modelling DW-MRI data from primary and metastatic ovarian tumours, European Radiology. 25 (2015) 2033–2040. doi:10.1007/s00330-014-3573-3.

[25] T. Takahara, Y. Imai, T. Yamashita, S. Yasuda, S. Nasu, M. Van Cauteren, Diffusion weighted whole body imaging with background body signal suppression (DWIBS): technical improvement using free breathing, STIR and high resolution 3D display., Radiat Med. 22 (2004) 275–282.

[26] K. Michielsen, I. Vergote, K. Op de beeck, F. Amant, K. Leunen, P. Moerman, C. Deroose, G. Souverijns, S. Dymarkowski, F. De Keyzer, V. Vandecaveye, Whole-body MRI with diffusion-weighted sequence for staging of patients with suspected ovarian cancer: a clinical feasibility study in comparison to CT and FDG-PET/CT, Eur Radiol. 24 (2014) 889–901. doi:10.1007/s00330-013-3083-8.

[27] S. Dhanda, M. Thakur, R. Kerkar, P. Jagmohan, Diffusion-weighted Imaging of Gynecologic Tumours: Diagnostic Pearls and Potential Pitfalls, RadioGraphics. 34 (2014) 1393–1416. doi:10.1148/rg.345130131.

[28] M. Torkzad, N. Casta, A. Bergman, H. Ahlström, L. Påhlman, H. Mahteme, Comparison between MRI and CT in prediction of peritoneal carcinomatosis index (PCI) in patients undergoing cytoreductive surgery in relation to the experience of the radiologist: MRI and CT for Prediction of PCI, Journal of Surgical Oncology. 111 (2015) 746–751. doi:10.1002/jso.23878.

[29] R.N. Low, R.M. Barone, J. Lucero, Comparison of MRI and CT for Predicting the Peritoneal Cancer Index (PCI) Preoperatively in Patients Being Considered for Cytoreductive Surgical Procedures, Ann. Surg. Oncol. 22 (2015) 1708–1715. doi:10.1245/s10434-014-4041-7.

[30] P. De Iaco, A. Musto, L. Orazi, C. Zamagni, M. Rosati, V. Allegri, N. Cacciari, A. Al-Nahhas, D. Rubello, S. Venturoli, S. Fanti, FDG-PET/CT in advanced ovarian cancer staging: Value and pitfalls in detecting lesions in different abdominal and pelvic quadrants compared with laparoscopy, European Journal of Radiology. 80 (2011) e98–e103. doi:10.1016/j.ejrad.2010.07.013.

[31] S. Schmidt, R.A. Meuli, C. Achtari, J.O. Prior, Peritoneal carcinomatosis in primary ovarian cancer staging: comparison between MDCT, MRI, and 18F-FDG PET/CT., Clin Nucl Med. 40 (2015) 371–377. doi:10.1097/RLU.0000000000000768.

[32] R.N. Low, R.M. Barone, Combined diffusion-weighted and gadolinium-enhanced MRI can accurately predict the peritoneal cancer index preoperatively in patients being considered for cytoreductive surgical procedures, Ann. Surg. Oncol. 19 (2012) 1394–1401. doi:10.1245/s10434-012-2236-3.

[33] M. Rosendahl, P. Harter, S.F. Bjørn, C. Høgdall, Specific Regions, Rather than the Entire Peritoneal Carcinosis Index, are Predictive of Complete Resection and Survival in Advanced Epithelial Ovarian Cancer, Int. J. Gynecol. Cancer. 28 (2018) 316–322. doi:10.1097/IGC.0000000000001173.

[34] K.L.M. Michielsen, I. Vergote, R. Dresen, K. Op de Beeck, R. Vanslembrouck, F. Amant, K. Leunen, P. Moerman, S. Fieuws, F. De Keyzer, V. Vandecaveye, Whole-body diffusion-weighted magnetic resonance imaging in the diagnosis of recurrent ovarian cancer: a clinical feasibility study, BJR. 89 (2016) 20160468. doi:10.1259/bjr.20160468.

[35] M. Espada, J.R. Garcia-Flores, M. Jimenez, E. Alvarez-Moreno, M. De Haro, L. Gonzalez-Cortijo, G. Hernandez-Cortes, V. Martinez-Vega, R. Sainz De La Cuesta, Diffusion-weighted magnetic resonance imaging evaluation of intra-abdominal sites of implants to predict likelihood of suboptimal cytoreductive surgery in patients with ovarian carcinoma, Eur Radiol. 23 (2013) 2636–2642. doi:10.1007/s00330-013-2837-7.

[36] J. Fehniger, S. Thomas, E. Lengyel, C. Liao, M. Tenney, A. Oto, S.D. Yamada, A prospective study evaluating diffusion weighted magnetic resonance imaging (DW-MRI) in the detection of peritoneal carcinomatosis in suspected gynecologic malignancies, Gynecologic Oncology. 142 (2016) 169–175. doi:10.1016/j.ygyno.2016.04.018.

[37] K. Michielsen, R. Dresen, R. Vanslembrouck, F. De Keyzer, F. Amant, E. Mussen, K. Leunen, P. Berteloot, P. Moerman, I. Vergote, V. Vandecaveye, Diagnostic value of whole body diffusion-weighted MRI compared to computed tomography for pre-operative assessment of patients suspected for ovarian cancer, European Journal of Cancer. 83 (2017) 88–98. doi:10.1016/j.ejca.2017.06.010.

[38] M.-A. Berthelin, M. Barral, C. Eveno, P. Rousset, R. Dautry, M. Pocard, P. Soyer, A. Dohan, Preoperative assessment of splenic involvement in patients with peritoneal carcinomatosis with CT and MR imaging, European Journal of Radiology. 110 (2019) 60–65. doi: 10.1016/j.ejrad.2018.11.022.

[39] B. Li, Q. Li, W. Nie, S. Liu, Diagnostic value of whole-body diffusion-weighted magnetic resonance imaging for detection of primary and metastatic malignancies: A meta-analysis, European Journal of Radiology. 83 (2014) 338–344. doi:10.1016/j.ejrad.2013.11.017.

Table 1

PRIMARY ACQUISITION	**DWIBS**	**T2TSE**	**3DT1GE**	
Orientation:	Coronal	Axial, coronal	Axial, coronal	Axial
Coverage:	Head – mid thigh	Head – mid thigh	Abdomen – pelvis	Chest
Repetition time (TR):	4736	1000	5.9	3.7
Echo Time (TE):	78	80	1.8	1.76
Flip angle			15^{o}	10^{o}
Number of signal Average (NSA):	4	1	1	1
FOV (RL×AP×CC) (mm):	450 × 230 × 300	498 × 230 × 400	400 × 352 × 230	400 × 359 × 230
Station Number:	3	4	2	1
Slice Thickness (ST) (mm):	6	6	4	4
Slice Number (SN) Coronal:	40	35	120	
Slice Number (SN) Axial:		140	120	115
Slice Spacing (mm):	0	1	0	0
Acquired voxel size (RL×AP×CC):	3.5 × 3.5	2 × 1.6	2 × 2 × 4	2.56 × 2.56 × 4
Reconstructed voxel size :	1.76	1.04	1× 1 × 2	1× 1 × 2
Respiration	Free	Triggered	Breathold	Breathold
Parallel imaging factor (SENSE)	4	2	2 × 1.3	2 × 1.3
Fat suppression			SPAIR (mDIXON)	SPAIR (eTHRIVE)
b values (s/mm^2)	0-1000			
DERIVED IMAGES		**Color fusion (DW overlay)**	**Color fusion (DW overlay)**	
	MIP Axial, sagital 3D Volumetric Coronal	Coronal	Axial, coronal	

Table 2

Age *(years)	mean, (sd)	56.00	(12.69)
Time to surgery (days)	median, (range)	12	(37)
CA-125 prior surgery (U/ml)	Median,(range)	167.5	(11760.8)
Primary site		Total (n=50)	
	Ovary	38	
	Fallopian tube	1	
	Uterus	2	
	Cervix	3	
	Other non-malignant Gynecologic	3	
	Other malignant non-Gynecologic	3	
Disease stage	**FIGO**	Total (n=50)	
	IA	8	
	IB1	1	
	IC1	1	
	IIA	1	
	IIB	1	
	IIIA1	1	
	IIIC	9	
	IV	2	
	N/A	5	
	Recurrent	21	
Histology		Total (n=50)	
	Serous adenocarcinoma	28	
	Clear cell	4	
	Mixed Müllerian Malignant Tumor (MMMT)	3	
	Serous cystadenoma	2	
	Endometriosis	2	
	Borderline Tumor	2	
	Endocervical Adenocarcinoma	1	
	Breast Adenocarcinoma	1	
	Biliary adenocarcinoma	1	
	Endometrioid Adenocarcinoma	2	
	Adenosarcoma	1	
	Leiomyoma	1	
	Gastro Intestinal Stromal Tumor (GIST)	1	
	Borderline Mucinous Tumor	1	
Surgical outcome		Total (n=50)	
	Microscopic (Complete)	39	
	Macroscopic <1 cm (Optimal)	7	
	Macroscopic >1 cm (Suboptimal)	4	

Table 3

Peritoneal cavity	Observer	TP	TN	FP	FN	Sensitivity	Specificity	PPV	NVP	Accuracy	Kappa
0 Central	R1	20	23	2	5	0,8	0,92	0,91	0,82	0,86	0,41
	R2	11	24	1	14	0,44	0,96	0,92	0,63	0,7	
1 Right upper	R1	18	25	4	3	0,86	0,86	0,82	0,89	0,86	0,63
	R2	14	24	5	7	0,67	0,83	0,74	0,77	0,76	
2 Epigastrum	R1	6	39	3	2	0,75	0,93	0,67	0,95	0,9	0,22
	R2	2	36	6	6	0,25	0,86	0,25	0,86	0,76	
3 Letf upper	R1	11	33	5	1	0,92	0,87	0,69	0,97	0,88	0,8
	R2	9	35	3	3	0,75	0,92	0,75	0,92	0,88	
4 Left flank	R1	7	37	5	1	0,88	0,88	0,58	0,97	0,88	0,61
	R2	5	36	6	3	0,63	0,86	0,45	0,92	0,82	
5 Left lower	R1	6	32	6	6	0,5	0,84	0,5	0,84	0,76	0,34
	R2	4	30	8	8	0,33	0,79	0,33	0,79	0,68	
6 Pelvis	R1	40	6	3	1	0,98	0,67	0,93	0,86	0,92	0,51
	R2	32	5	4	9	0,78	0,56	0,89	0,36	0,74	
7 Right lower	R1	11	32	4	3	0,79	0,89	0,73	0,91	0,86	0,27
	R2	8	30	6	6	0,57	0,83	0,57	0,83	0,76	
8 Right flank	R1	17	27	3	3	0,85	0,9	0,85	0,9	0,88	0,47
	R2	11	27	3	9	0,55	0,9	0,79	0,75	0,76	
9 Upper jejunum	R1	4	44	2	0	1	0,96	0,67	1	0,96	0,4
	R2	2	45	1	2	0,5	0,98	0,67	0,96	0,94	
10 Lower jejunum	R1	3	45	2	0	1	0,96	0,6	1	0,96	0,15
	R2	1	44	3	2	0,33	0,94	0,25	0,96	0,9	
11 Upper Ileum	R1	4	43	2	1	0,8	0,96	0,67	0,98	0,94	0,12
	R2	2	43	2	3	0,4	0,96	0,5	0,93	0,9	
12 Lower Ileum	R1	9	35	3	3	0,75	0,92	0,75	0,92	0,88	0,38
	R2	5	35	3	7	0,42	0,92	0,63	0,83	0,8	
Summary	**R1**	**156**	**421**	**44**	**29**	**0,84**	**0,89**	**0,72**	**0,92**	**0,89**	**0,41**
	R2	**106**	**414**	**51**	**79**	**0,51**	**0,87**	**0,6**	**0,81**	**0,8**	
						p<0,001	**p=0,151**	**p=0,006**	**p<0,001**	**p<0,001**	

Figure 1
Click here to download high resolution image

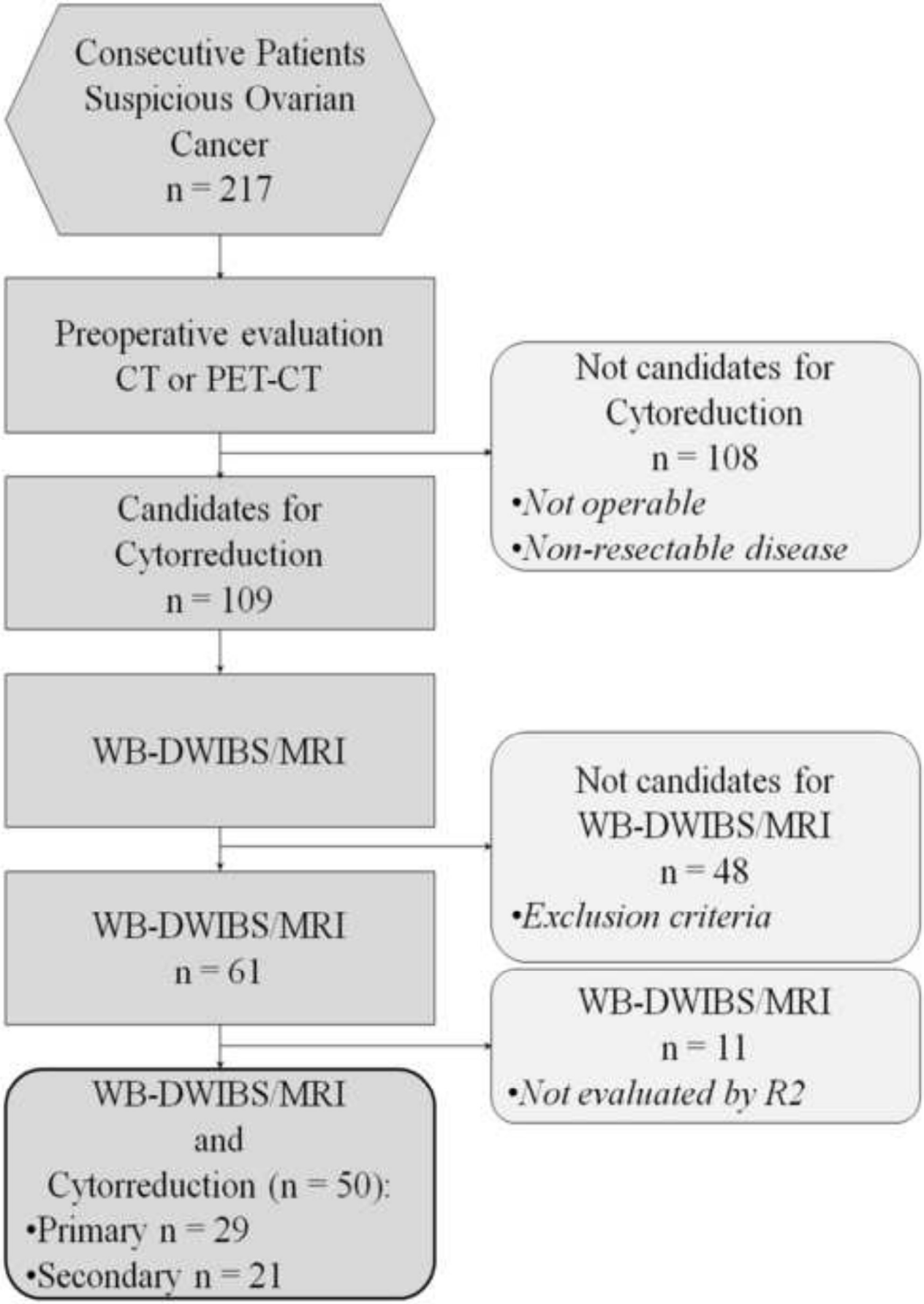

Figure 2
Click here to download high resolution image

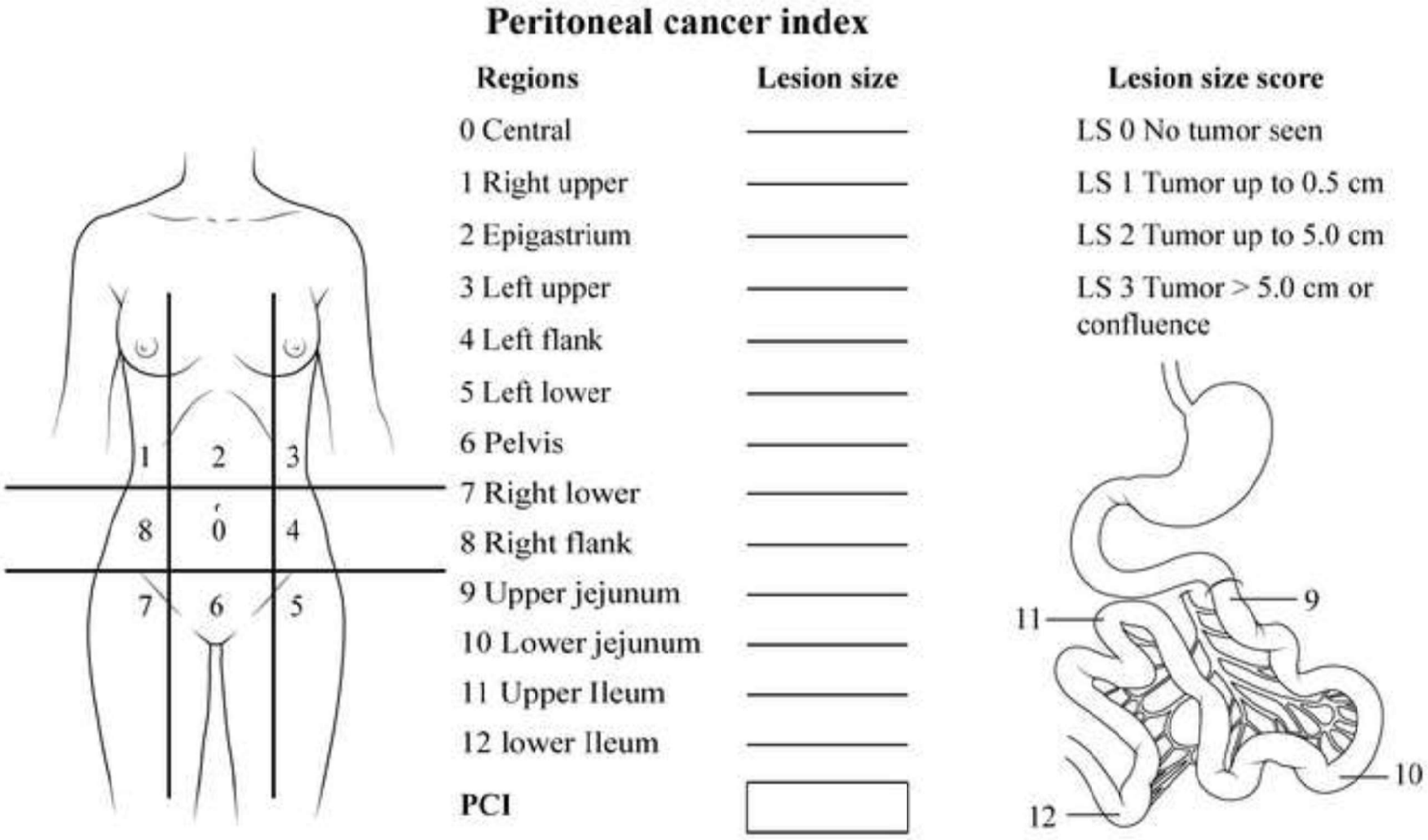

Figure 3

Click here to download high resolution image

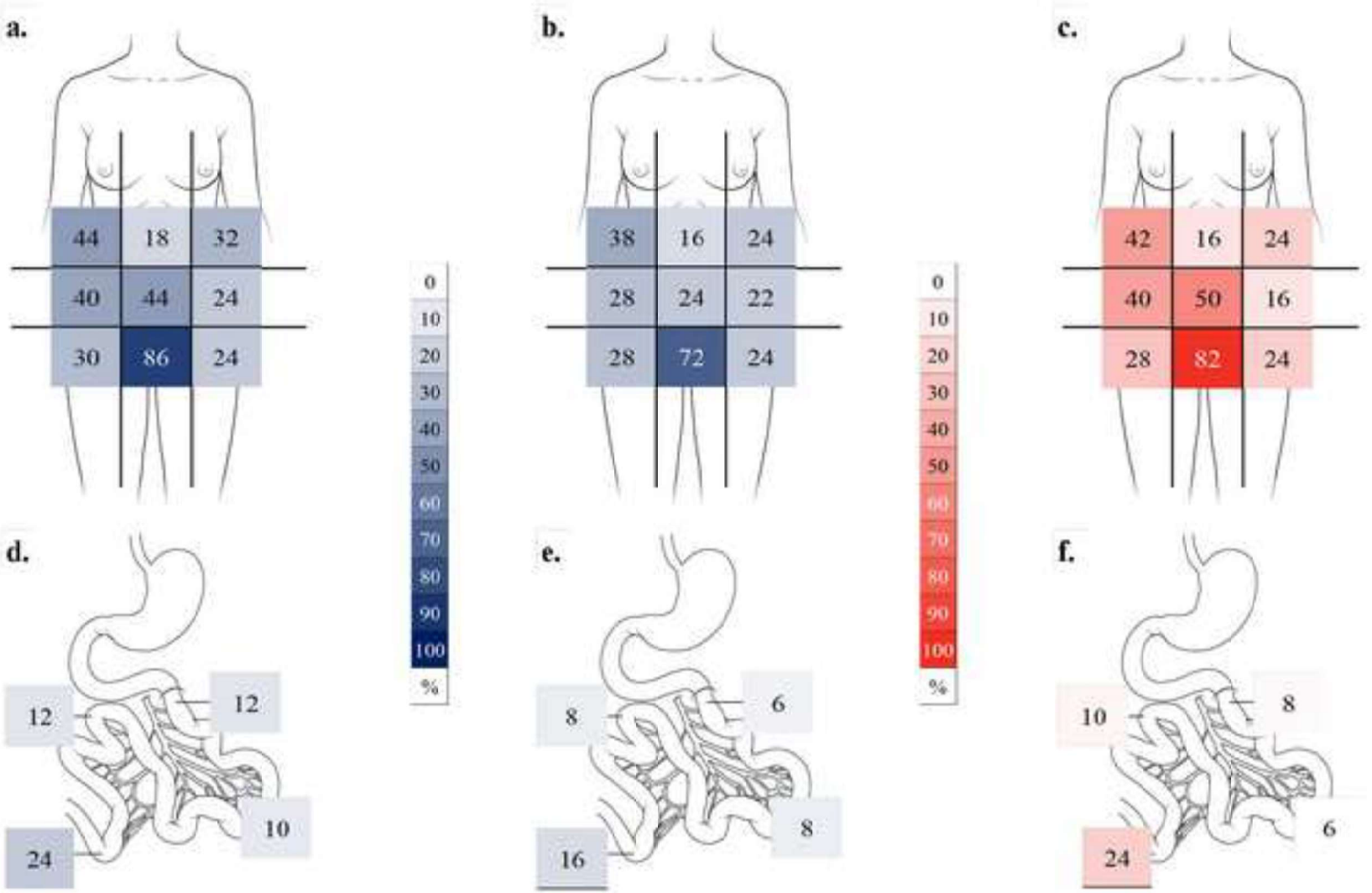

Figure 4

Click here to download high resolution image

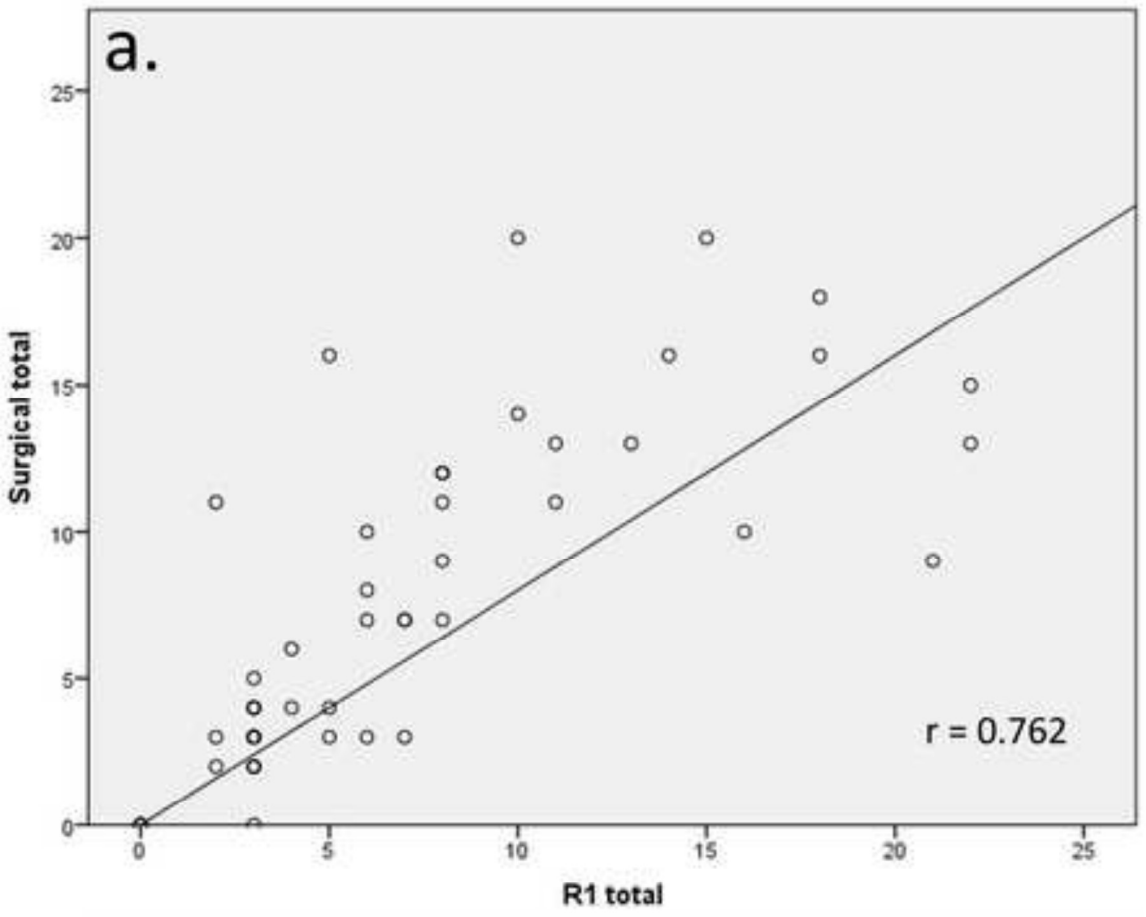

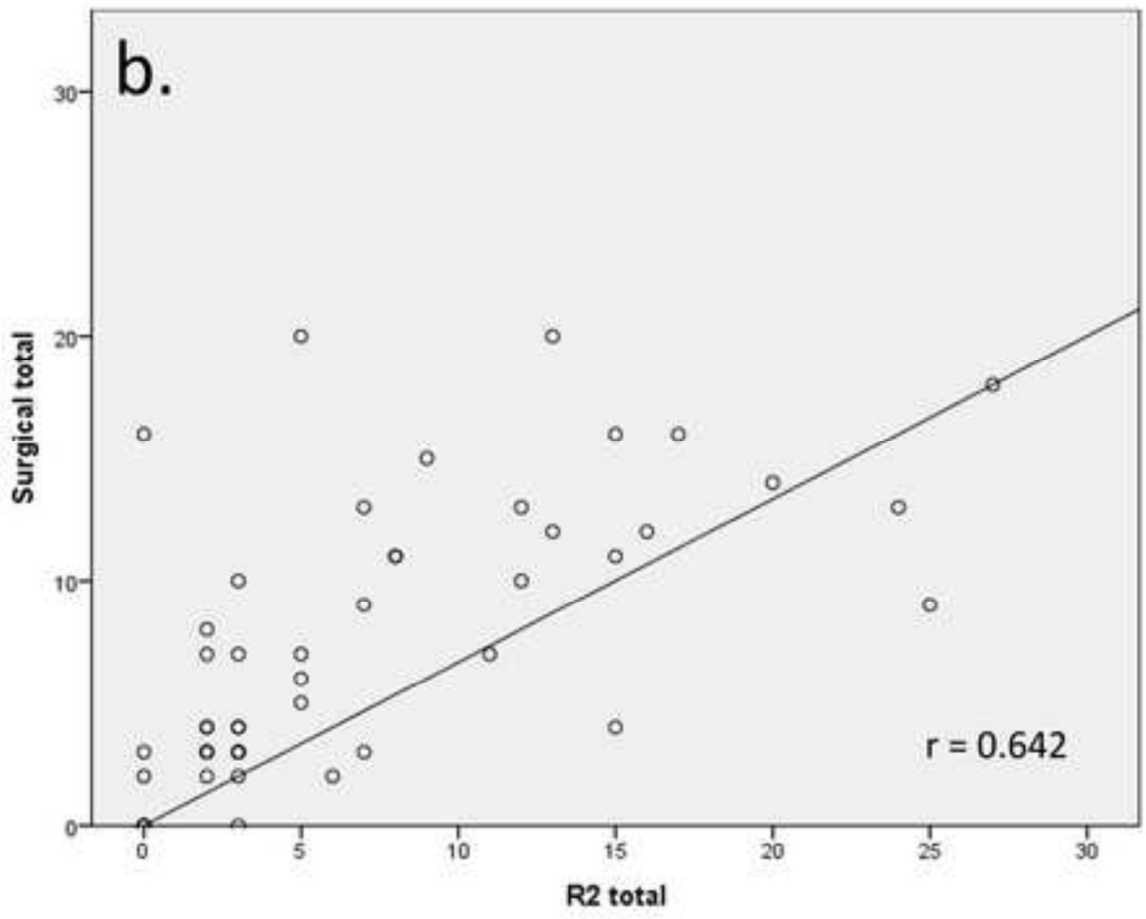

Figure 5
Click here to download high resolution image

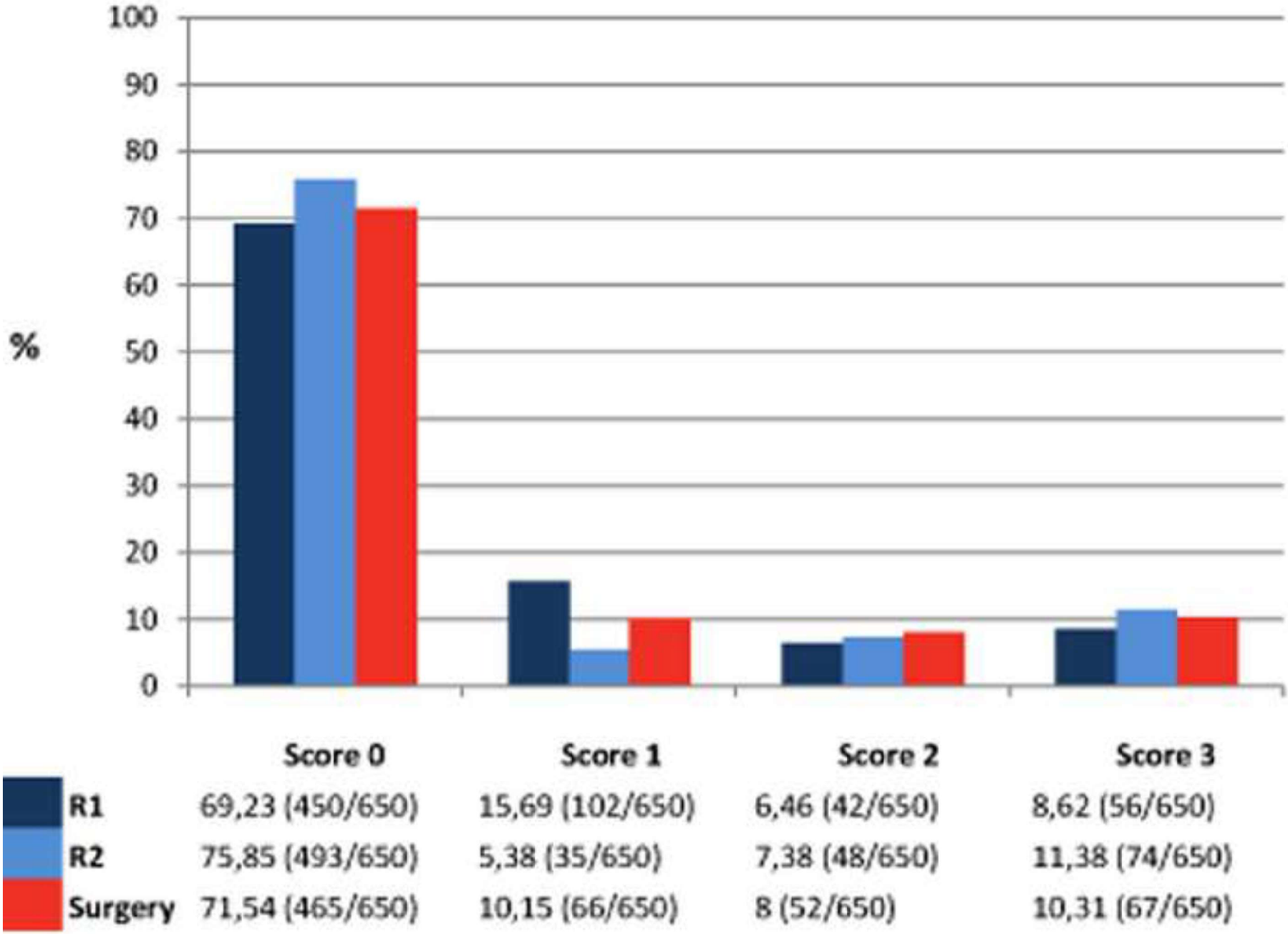

Figure 6

Click here to download high resolution image